Transactions of the Materials Research Society of Japan 29 [8] 3519-3522 (2004)

A comparison of microstructural refinement of Al by three different severe plastic deformation techniques

A. Godfrey, W.Q. Cao, W. Liu and Q. Liu
Dept. Materials Science and Engineering, Tsinghua University, Beijing 100084, China.
Fax: 86-10-6277-1160, e-mail: awgodfrey@bigfoot.com

The microstructural refinement during severe plastic deformation of aluminium by three different processing routes (equal angle channel extrusion (ECAE), accumulated roll-bonding (ARB), and high-strain conventional rolling (HSCR)), has been investigated. ECAE processing (route Bc) leads to heterogenous microstructures, with mixed regions of good and poor refinement. Room temperature ARB (using lubrication) gives homogeneous refinement, though not as good as the best parts of the ECAE samples. HSCR is not suitable for production of fine-grained bulk samples. The annealing behaviour depends both on the fraction of high angle boundaries in the deformed material, and on the heterogeneity of the deformation microstructure. For ARB the presence of oxide particles also affects the annealing response. The flow stress (estimated from hardness measurements) has been compared to the stored energy (calculated from microstructural measurements of boundary spacings and misorientation angles) for both annealed and deformed samples. When normalized by the friction stress the curves for all three routes overlap, suggesting that there are no fundamental differences in mechanisms for the different production routes.

Key words: ECAE, ARB, aluminium, severe plastic deformation.

1. INTRODUCTION

Much interest exists currently in severe plastic deformation (SPD) of bulk metallic samples to large plastic strains by a variety of processes. The main interest in SPD processing is in the production of materials with very fine (ideally less than 1μm) grain sizes, to take advantage of the large increases in mechanical strength available, according to the Hall-Petch relationship, for grain sizes in the near micron range. Additionally, it has been shown by a number of authors that the fine grain sizes achievable by SPD processing can produce materials suitable for super-plastic processing.

Many different SPD processing techniques have now been suggested. The techniques can be broadly split into those that rely mostly on repeated application of a shearing-mode deformation, and those that use repeated application of a plane-strain deformation. The most common example of the former is the equal channel angle extrusion (ECAE) process [1,2] The second group is largely described by the accumulated roll-bonding (ARB) process – a variant of conventional rolling, where after each rolling step the sample is cut in half and then stacked vertically, before being given the next rolling pass [3,4]. It is important to note however that in most cases some combination of shear and plane-strain deformation takes place [4,5]. The mechanism for the microstructural refinement during SPD processing relies on the agglomeration into boundaries of dislocations introduced during the plastic deformation. The major parameters describing the extent of the microstructural refinement are therefore, as for metals deformed to conventional strains, the average dislocation boundary spacing and the average misorientation (crystal rotation) across the dislocation boundaries [6,7]. These parameters are also the most important for determining the mechanical strength (flow stress) of the processed material [8]. Whereas the flow stress of a fully recrystallized material can be described by the average grain size, in materials produced by SPD processing the microstructures contain a mixture of both high and low misorientation angle boundaries. It is of interest therefore to examine parameters that include both the dislocation boundary spacing and misorientation, and to investigate the use of such parameters for comparing the effectiveness of different SPD processing routes. For dislocation cell forming materials, one such parameter is the stored energy of deformation, as the energy can be expressed as a product of a misorientation dependant boundary energy and an inverse boundary spacing.

For practical use, annealing of SPD samples is usually required to restore some material ductility. In order to achieve a fine control of the grain size, the thermal stability of the deformed structure is, therefore, also an important consideration. It has been suggested that the details of the deformation microstructure are also important for determining whether annealing results in a discontinuous recrystallization, or a continuous subgrain growth process [9].

In this study microstructural measurements on samples deformed by ECAE, ARB and high-strain cold rolling (HSCR) are reported. The results are used to explore the relationship between flow-stress and stored energy for each processing route. The annealing behaviour of samples deformed by each route is also compared.

2. FLOW STRESS AND STORED ENERGY

An empirical relationship between stored energy and flow stress can developed from the following two well

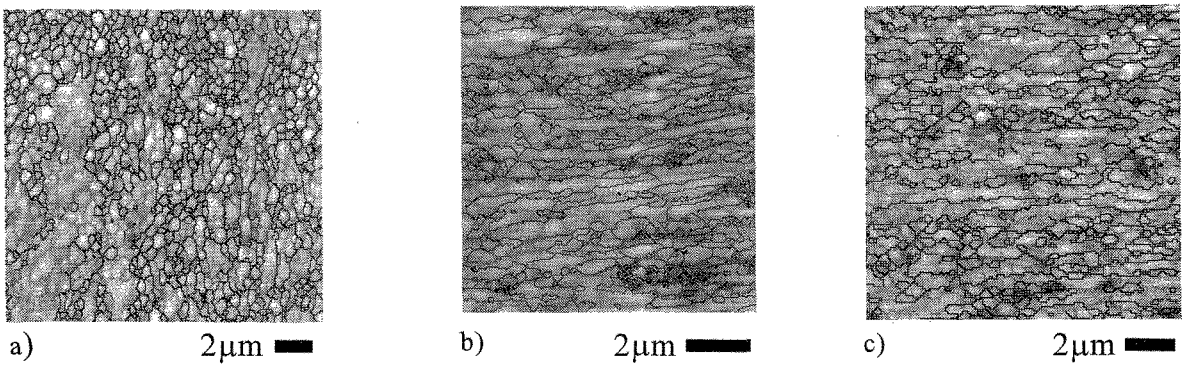

Fig.1: EBSP orientation image maps showing deformed microstructures. Black and grey lines represent misorientations of >15° and 1.5° respectively. The background contrast is related to the EBSP quality at each map pixel: a) ECAE, $\varepsilon \approx 10$ (transverse section); b) ARB, $\varepsilon \approx 4$ (longitudinal section); c) HCSR, $\varepsilon \approx 4$ (longitudinal section). For (b) and (c) the scale-bars are parallel to the rolling direction.

known relationships:

$$E_S = K\rho Gb^2 \quad (1)$$
$$\sigma - \sigma_0 = M\alpha Gb\rho^{0.5} \quad (2)$$

where E_S is the energy stored due to dislocations, ρ is the dislocation density, G is the shear modulus, b is the Burgers vector, σ is the flow stress, σ_0 is the friction stress, M is the Taylor factor, and K and α are numbers approximately equal to 0.5 and 0.24 respectively. Combining these equations gives

$$\sigma = \sigma_0 + M\alpha(G/K)^{0.5}(E_S)^{0.5} \quad (3)$$

i.e. the flow stress depends upon the square root of the stored energy. The validity of this expression is well known for the low strain regime where dislocations can be thought of as being uniformly distributed throughout a sample. For higher strains the energy is more suitably expressed by an expression of the form, $E_S = S_V E_A(\theta)$ where $E_A(\theta)$ represents the energy per area of a boundary with misorientation θ, and S_V is the area per unit volume of those boundaries. We assume here that the dislocation boundaries are perfect rotation boundaries such that $E_A(\theta)$ is given by the Read-Shockley function, and that the free dislocation content (ρ_0) can be neglected.

3. EXPERIMENTAL METHODS

Samples deformed by three different processes were investigated: (i) ECAE of Al-1050, using route Bc with a 90° die; (ii) ARB of Al-1100, carried out at room temperature with lubrication; (iii) high strain multi-pass rolling of Al-1200. Samples were sectioned in the longitudinal and transverse planes. Orientation maps using step-sizes of between 50nm and 200nm were generated from electro-polished samples, using a field emission gun scanning electron microscope (FEG-SEM) equipped with an electron back-scatter pattern (EBSP) analysis system.

The average dislocation cell size ($d_{av(\theta>1.5°)}$) was measured using a reconstruction method, using a boundary misorientation threshold of 1.5°. At this value the data are still affected by the angular resolution of the EBSP technique, resulting in a large number of very small artificial dislocation cells. The data were further processed by identifying all reconstructed cells with an area below 0.01μm², then re-assigning these areas with the orientations of neighbouring larger dislocation cells. The procedure is described in detail in [11]. Average boundary misorientations ($\theta_{av(\theta>1.5°)}$) were calculated from the (adjusted) reconstructed dislocation cell structures. The flow-stress was estimated from micro-hardness measurements, taken using a load of 50g. For each sample a total of at least 8 measurements were made. Annealing was carried out at different temperatures for a duration of 2 hours, using an air-furnace.

4. RESULTS

4.1 Deformed microstructures

Typical EBSP orientation maps for samples deformed to strains of $\varepsilon \approx 4$ (ARB and HSCR) and $\varepsilon \approx 10$ (ECAE) are shown in Fig. 1(a-c). In these maps misorientations of >1.5° and 15° are shown by grey and black lines, respectively. The background contrast corresponds to the EBSP quality at each map pixel. Differences between the samples are seen both in the dislocation cell shapes and in the heterogeneity of the deformed microstructure.

4.2 Dislocation boundary spacing and misorientation

The variation of average dislocation cell size ($d_{av(\theta>1.5°)}$) and of average misorientation ($\theta_{av(\theta>1.5°)}$) as a function of accumulated strain is shown for each SPD process in Fig. 2(a,b). The average spacing continuously decreases for ARB and HSCR, whereas for ECAE the data tend to show a leveling off in the average spacing. In contrast ARB and ECAE samples show a similar continuous increase of average misorientation with increasing strain.

4.3 Dependence of flow stress on stored energy

For each sample condition the value of E_S was calculated from the measured values of $d_{av(\theta>1.5°)}$ and $\theta_{av(\theta>1.5°)}$ according to

$$E_S = (2/d).\gamma_m(\theta/\theta_m)[1-\ln(\theta/\theta_m)] \quad : \theta<15°$$
$$E_S = (2/d).\gamma_m \quad : \theta\geq15° \quad (4)$$

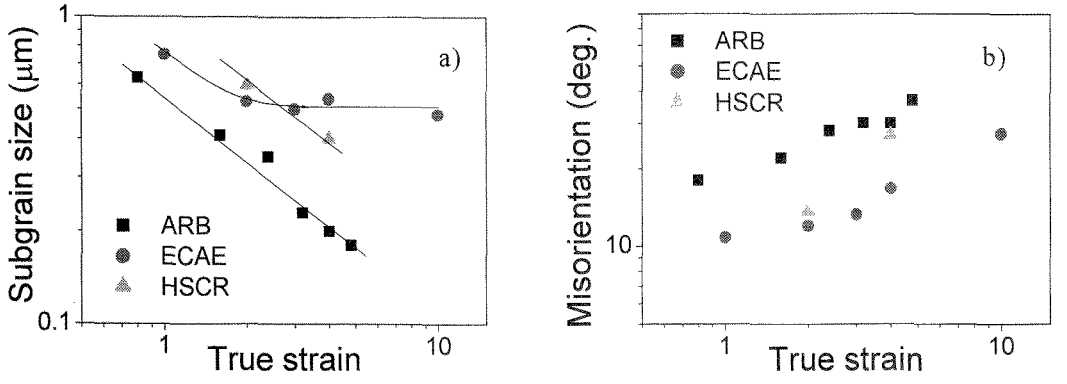

Fig.2: Variation of microstructural parameters for the three different processing routes, as determined from EBSP investigations: a) subgrain size (defined as the average spacing of boundaries >1.5°); b) average misorientation of boundaries >1.5°.

where d and θ represent the average values of dislocation boundary spacing and misorientation. The values for γ_m and θ_m were taken as 0.324Jm^{-2} and 15° respectively.

The data are plotted in Fig. 3a as $E_S^{0.5}$ against the flow stress, as estimated from hardness measurements. For each process a linear fit is observed, showing that a relationship between flow stress and stored energy of deformation also holds at high strains.

The alloy composition used for each processing route differs slightly (both initially, and for the case of the ARB samples, as a result of the introduction of an oxide phase during processing). In order therefore to allow an easier comparison of the results, the data for each of the three processing routes have been normalized by subtraction of the effective friction stress (taken from the y-intercept at $E_S^{0.5} = 0$). The results (Fig. 3b) demonstrate clearly that for each process the same relationship exists between hardness and the stored energy of deformation.

4.4 Annealing behaviour for each SPD processing route

Significant differences were observed in the annealing behaviour of samples deformed by each of the three SPD methods (differences were also observed between low and high strain deformed samples for each process – here we only consider annealing of samples deformed to strains of above $\varepsilon \approx 4$). Figure 4 shows examples of annealed microstructures for the three different SPD routes. In the ECAE material some parts of samples show changes typical of a discontinuous recrystallization process, whilst in other parts of the sample a more uniform coarsening of the microstructure is seen. In the HSCR samples, for all strains annealing results only in discontinuous recrystallization. In the ARB samples the annealed microstructure is clearly influenced by the presence of oxide stringers along regions corresponding to the interfaces formed between the sheets during the ARB processs.

5. DISCUSSION

5.1 Dislocation storage during deformation

The combined flow-stress vs. $E_S^{0.5}$ (Fig. 3b) show that the data for several different processes can be reduced to a single master curve. In the calculation we have ignored the possible contribution of free (loose) dislocations to the stored energy ($E(\rho_0)$). The fit, however, of the data shows that any such contribution to the stored energy must be proportional to $E_S^{0.5}$. The existence of a master curve suggests that no fundamental difference in dislocation storage mechanism exists between the different SPD processes. An interesting test of this idea

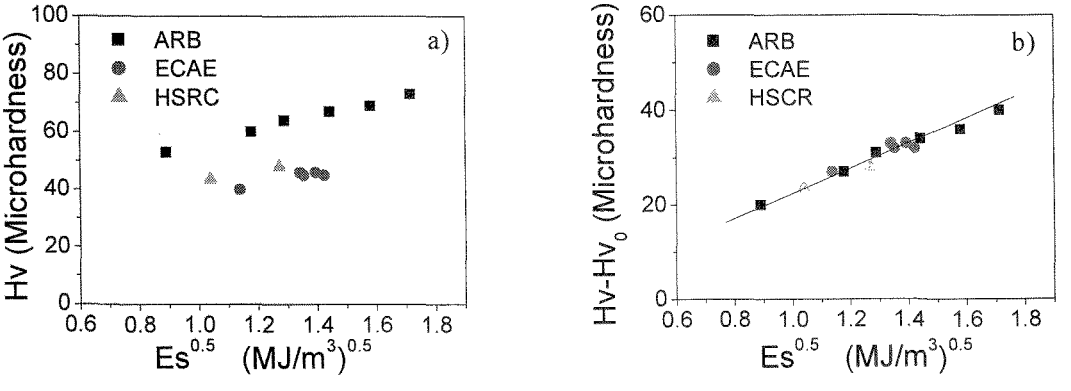

Fig.3: Variation of Vickers hardness with the square root of the stored energy due to the dislocation substructure. The stored energy, E_S, is calculated from the microstructural parameters according to Eqn. 4: a) ARB, ECAE and HSCR measurements; b) the data for each material are normalized by subtraction of the friction stress (Hv_0) to show that all points fall on a single line.

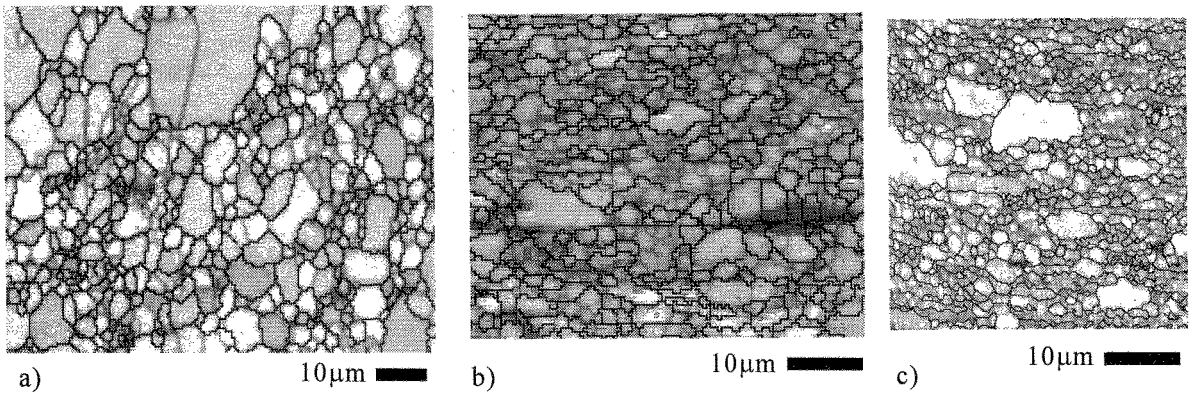

Fig.4: EBSP orientation image maps showing annealed microstructures. Black and grey lines represent misorientations of >15° and 1.5° respectively. The background contrast is related to the EBSP quality at each map pixel: a) ECAE ε = 10, 270°C for 2 hours (transverse section); b) ARB ε = 4, 260°C for 2 hours (longitudinal section); c) HCSR ε = 4, 260°C for 2 hours (longitudinal section).

will be to investigate whether data for recovered samples (in which some changes in the dislocation configurations are expected to take place) give results that fall on the same master curve.

5.2 Heterogeneity of deformation

Microstructural observations show that whilst all three processes lead to microstructural refinemement, there are differences in the both the morphology and the homogeneity of the deformed microstructures. The most visible difference is the much greater heterogeneity of the ECAE microstructures. This heterogeneity results in a situation where at a given strain the most refined regions are seen in the ECAE samples, but where on average the ARB route gives a more refined microstructure.

Whilst these heterogeneities are not reflected in the relationship between mechanical strength and stored energy, they lead to differences in the annealing response of the materials. Theoretically the annealing of a deformed metal can result in two types of behaviour: (i) discontinuous recrystallization, corresponding to the movement of a high angle boundaries through only slightly recovered deformed material; or (ii) continuous coarsening (sometimes referred to as extended recovery), where the structure evolves in a manner similar to grain growth. Continuous coarsening is preferable for SPD materials as such behaviour allows a much greater control of the grain size, allowing a balance between ductility improvement and loss of mechanical strength.

For the HSCR material annealing leads in all cases to a clear discontinuous recrystallization process (the early stages of which are seen in Fig. 4c). For the ECAE and ARB materials the situation is not so straightforward. The ECAE material shows mixed behaviour: in some places very large grains are seen (resulting from discontinuous type behaviour), whereas in other places the a more continuous evolution of the microstructure is observed. The heterogeneous annealing behaviour is likely to result directly from the heterogeneity in the deformation microstructure. In the ARB material the annealing behaviour is again mixed. The development of very large grains is however limited in places by oxide particles introduced during the processing. For both ECAE and ARB the annealing response is therefore affected both by microscopic and macroscopic parameters.

ACKNOWLEDGEMENTS

This work was supported by the National Natural Science Foundation of China under contract nos: 59825110 and 50231030. Samples were kindly provided by Dr. Z. Horita, Kyushu University (ECAE), Dr. N. Tsuji, Osaka University (ARB), and Alcan International (HSCR).

REFERENCES

[1] Y. Iwahashi, Z. Horita, M. Nemoto and T. G. Langdon, *Acta mater.*, 46, 3317-3331 (1998).
[2] R. Z. Valiev, R. K. Islamgaliev and I. V. Alexandrov, *Prog. Mater. Sci.*, 45, 103-189 (2000).
[3] Y. Saito, N. Tsuji, H. Utsunomiya, T. Sakai and Hong, *Scripta mater.*, 39, 1221-1227 (1998) .
[4] N. Tsuji, Y. Ito, Y. Saito and Y. Minamino, *Scripta mater.*, 46, 893-899 (2002).
[5] A. Gholinia, P. B. Prangnell and M. V. Markushev, *Acta Mater.*, 48, 1115-1130 (2000).
[6] D. A. Hughes, Q. Liu, D. C. Chrzan amd N. Hansen, *Phys. Rev. Lett.*, 81, 4664–4667 (1998).
[7] A. Godfrey and D. A. Hughes, *Acta mater.*, 48, 1897-1905 (2000).
[8] D. A. Hughes and N. Hansen, *Acta mater.*, 48, 2985-3004 (2000).
[9] F. J. Humphreys, P. B. Prangnell, J. R. Bowen, A. Gholinia and C. Harris, *Phil. Trans. R. Soc. Lond.*, 357, 1663 (1999).
[10] W. Q. Cao, A. Godfrey and Q. Liu, *J. Microsc.*, 211(3), 219-229 (2003).

(Received December 1, 2003; Accepted June 23, 2004)